Theoretical Study of $V^{2+}OH_2/V^{3+}OH_2$ Electron Transfer Reactivity at Electron Correlation Level

Yuxiang Bu,*,†,‡ Xinyu Song,‡ and Chengbu Liu†

Institute of Theoretical Chemistry, Shandong University, Jinan, 250100, China, and Department of Chemistry, Qufu Normal University, Qufu, 273165, China

Received: November 19, 1998

A novel theoretical model for discussing the electron transfer reactivity is presented in this paper and also is calibrated in terms of the monohydrated vanadium ion system, $V^{2+}OH_2/V^{3+}OH_2$. The detailed calculations have been made at the UMP2(full)/6-311+G* level. The relevant energy quantities (such as the activation energy, dissociation energy, et al.) have also been obtained at different levels of theory (HF, MP2, MP3, MP4, and QCISD and corresponding spin-projection PUHF, PMP2, and PMP3) with the same basis set (6-311+G*) and valence electron correlation. The electronic transmission coefficient is calculated using the ab initio potential energy surface slopes, and the coupling matrix element determined from the two-state model and the Slater-type d-electron wave functions. The relevant kinetic parameters are obtained in terms of new schemes presented in this paper. The contact distance dependence of these parameters and the applicability of the presented models are also discussed.

1. Introduction

Electron transfer (ET) reactions in solution are very complicated reactions,[1−9] not only because there are many complicated surrounding factors which influence the ET rate and mechanism, but also because there are many structural factors from the reactant molecules themselves.[10−22] It is well-known that the transition metal coordination ions in solution keep some complex equilibrium. For the hydrated V^{2+} ion ($V^{2+}(aq)$), there coexist several coordination equilibria.

$$\begin{gathered} V^{2+} + H_2O \rightleftarrows V^{2+}OH_2 \\ V^{2+}OH_2 + H_2O \rightleftarrows V^{2+}(H_2O)_2 \\ V^{2+}(H_2O)_2 + H_2O \rightleftarrows V^{2+}(H_2O)_3 \\ V^{2+}(H_2O)_3 + H_2O \rightleftarrows V^{2+}(H_2O)_4 \\ V^{2+}(H_2O)_4 + H_2O \rightleftarrows V^{2+}(H_2O)_5 \\ V^{2+}(H_2O)_5 + H_2O \rightleftarrows V^{2+}(H_2O)_6 \\ V^{2+}(H_2O)_6 + (n\text{-}6)H_2O \rightleftarrows V^{2+}(H_2O)_n \ (n > 6) \end{gathered} \tag{1}$$

Therefore, there coexist various hydrated vanadium(II) $[V^{2+}(H_2O)_m]$ ($m = 0, 1, 2, 3$, etc.) in solution. Similar phenomena may also be observed for the hydrated vanadium(III) ion. Obviously, $V^{2+}(H_2O)$ and $V^{3+}(H_2O)$ are also important species and must play an important part in the ET process. Thus, it is very useful to investigate ET reactivity of these intermediate species in the complex equilibrium in solution for further approaching the experimentally observed statistically averaged ET rate. However, it is very difficult to determine experimentally the structures and reactivities of these intermediate species in solution phase; therefore, the high-level theoretical approaches are needed.

To theoretically investigate the structures and ET reactivities of these intermediate species, taking $V^{2+}OH_2/V^{3+}OH_2$ pairs as an example, in this paper, an accurate ab initio calculational scheme is presented for discussing the electron self-exchange reactivity at the electron correlation level. The relevant kinetic parameters in solution and also in gas phase are calculated. The distance dependence of these parameters, the electronic structures, and the properties of these species are also discussed.

2. Theoretical Schemes

In general, electron transfer can occur over a range of encounter distance, R_{M-M}, defined as metal−metal separation in the ion pair. Thus, for the following type of outer sphere electron exchange reaction involving transition metal ions

$$ML^{2+} + ML^{3+} \rightleftarrows ML^{3+} + ML^{2+} \tag{2}$$

The overall observed ET rate may be expressed as the following integral formalism. This weights $k_{et}(R_{MM})$ by $4\pi R_{MM}^2$ times the pair distribution function $g(R_{MM})$,[23,24]

$$k_{obs} = \int 4\pi R_{MM}^2 \, g(R_{MM}) \, k_{et}(R_{MM}) \, dR_{MM} \tag{3}$$

where $4\pi R_{MM}^2 \, g(R_{MM}) \, dR_{MM}$ is the differential equilibrium constant for precursor complexes with distances lying between R_{MM} and $R_{MM} + dR_{MM}$, $k_{et}(R_{MM})$ corresponds to the primary electron exchange rate at the encounter distance (R_{MM}). For the following process eq 4, $k_{et}(R_{MM})$ can be expressed as eq 5

$$ML^{2+}...ML^{3+} \rightleftarrows ML^{3+}...ML^{2+} \tag{4}$$

$$k_{et}(R_{MM}) = \kappa_{el}(R_{MM}) \, Z_{eff} \exp(-E_{ad}(R_{MM})/kT) \tag{5}$$

where Z_{eff} now refers to the combined "nuclear frequency factor" and κ_{el} is the electronic transmission factor. It becomes

† Shandong University.
‡ Qufu Normal University.

10.1021/jp984490h CCC: $18.00
Published on Web 05/20/1999

apparent that the electronic factor and activation energy are two key quantities affecting the ET rate, and these two factors depend strongly on the encounter distance. In this section some new schemes will be introduced with high-level ab initio calculations for the relevant kinetic parameters of the unimolecular reaction process and then for the pair distribution function.

(i) Activation Model. It should first be noted that there are two contributions to the total energy of the reacting system from the reduced and the oxidized species, both in the reactants state and in the products state. Therefore, the potential energy surface (PES) of the reactants or of the products may be obtained by summing the PES of the corresponding oxidized and reduced species. According to the modified self-exchange model,[10] considering the properties of the monohydrated transition metal ion redox system and using the one-dimensional linear reaction coordinate, the reactants state PES is

$$E_1 = E_r(q_r) + E_o(q_o) \tag{6}$$

After the electron transfer, the products state PES may be expressed as

$$E_2 = E_o(x-q_r) + E_r(x-q_o) \tag{7}$$

Obviously for the self-exchange reactions, according to the energy conservation during the transition ($E_1 = E_2$), the energy of the reacting system at the transition state is given by

$$E_{ad} = E_r(q_r) + E_o(x-q_r) \tag{8}$$

By minimizing the total activation potential energy surface (eq 8), the adiabatic activation energy may be obtained by

$$E_{ad} = E_r(q_r^t) + E_o(x-q_r^t) \tag{9}$$

where E_r and E_o denote the PES of the reduced and the oxidized species, x is the corresponding nuclear configuration displacement from the initial to the final states, and q_r^t is that of the reduced species at the transition state.

Equation 9 has shown that calculations of the activation energy depend strongly on the PES of the reacting system. However, it is very difficult to accurately determine the PES of the hydrated ion in solution. In this treatment, the hydrated ion is divided into the inner-sphere complex ion and the outer-sphere solvent medium: the inner-sphere part may be accurately calculated using ab initio method at the electron correlation level, and the outer-sphere part may be determined macroscopically.

(ii) Electronic Factor. The electronic coupling factor is a very important quantity affecting the ET rate. It, summarizing all electronic effects on the ET rate, may be generally expressed as

$$\kappa_{el} = 2P_0/(1 + P_0) \tag{10}$$

where P_0 is the electron adiabatic transition probability for hopping from the initial (i) to the final (f) diabatic PES on a single passage of the system through the crossing region. For the weak coupling system, P_0 may be obtained by using the Landau−Zener model.[25,26]

$$P_0 = 1 - \exp(-4\pi^2 H_{if}^2/(h\upsilon_s|S_2 - S_1|)) \tag{11}$$

where h is Planck's constant and υ_s is the thermally averaged velocity of the reacting system, $M^{2+}OH_2/M^{3+}OH_2$, along the reaction coordinate. S_1 and S_2 stand for the negative PES slopes of the reactants and the products with respect to the reaction coordinate.

A. The Coupling Matrix Element H_{if}. For this weak coupling system, H_{if} may be directly expressed as a simple formalism.

$$H_{if} = \langle\psi_f|H_{el}|\psi_i\rangle \tag{12}$$

where ψ_i and ψ_f are the initial state and the final state functions and H_{el} is the electronic Hamiltonian for the whole system.

A new method is presented in this calculation. Taking five d-type orbitals of the central metal ion in the free state as the orbital basis set, the initial state wave function ψ_i of a transferring electron in the hydrated vanadium(II) ion in solution is obtained in terms of the perturbation theory

$$\psi_i = \psi_d^{(1)}(r)Y_{lm}(r)$$

where $\psi_d^{(1)}$ is the first-order perturbed radial wave function of the 3d electron state in the hydrated vanadium(II) in solution, $Y_{lm}(r)$ is the spherical harmonic function that represents the angular part of the wave function ψ_i. In the perturbation calculations, the potential field produced by ligands and the outer-sphere solvent is taken as a perturbation potential. It is expressed in terms of the electrostatic potential between an electron and the ligand as

$$U = Q_O e^2/|r_O|^2 + Q_H e^2/|r_{H1}|^2 + Q_H e^2/|r_{H2}|^2 + U_{sol}(r_w) \tag{13}$$

here

$$U_{sol}(r_w) = Z_d\alpha e^2/2r_w^4 + eD\langle cos\theta\rangle/r_w^2 \tag{14}$$

where α is the polarizability, D is the dipole moment of the ligand (dipole), r_w is the M−L bond distance, and θ is the angle between the dipole direction and r_w. Q_O and Q_H are the net charges at oxygen and hydrogen atoms of the inner-sphere ligand, and r_{H1} and r_{H2} are the radial vectors of the 3d electron from atoms H(1) and H(2).

The first-order perturbed 3d state electron wave function can be obtained as

$$\psi_d^{(1)} = \sum_{m=1}^{5} C_m \psi_{dm}^{(0)} \tag{15}$$

where C_m relates to

$$\sum_{m=1}^{5} (H_{ml} - E_d^{(1)}\delta_{ml})C_m = 0 \tag{16}$$

$$H_{ml} = \langle\psi_{dm}^{(0)}|U|\psi_{dl}^{(0)}\rangle \tag{17}$$

Substitution of these electronic state functions into eq 12 can give the results of H_{if} by using the numerical integral method.

B. PES Slopes. In general approximate calculations, the $\upsilon_s|S_2 - S_1|$ in eq 11 was reduced to a simple formalism.[3,4,23]

$$|S_2 - S_1| = 8\omega_{eff}\sqrt{(\pi RTE_{ad})}/\upsilon_s \tag{18}$$

where ω_{eff} is the effective vibrational frequency. It is not appropriate to apply eq 18 in the accurate determination of the electronic transmission coefficient.

For a given PES, $E(Q)$, the slope can be obtained from the relationship

$$S_j = -\partial E_j(Q)/\partial Q \tag{19}$$

where $E_j(Q)$ is the PES of the reactants state ($j = 1$) or that of the products state ($j = 2$) as a function of the reaction coordinate, Q. Using the one-dimensional linear reaction coordinate, the slope difference $|S_2 - S_1|$ may be obtained by

$$|S_2 - S_1| = |-\partial E_2(q_o)/\partial q_o + \partial E_1(q_r)/\partial q_r| = 2|S_r - S_o| \tag{20}$$

where S_r and S_o denote the PES slopes of the reduced and the oxidized species at the transition state.

(iii) Pair Distribution Function. Aside from the electronic and activation factors, the electron transfer rate also depends on the encounter distance through the pair distribution factor, $g(R_{MM})$. This distribution function depends strongly on the interaction between two reacting species and may be approximately expressed as a function of a simple screened Coulombic repulsion.

$$g(R_{MM}) = \exp(-V(R_{MM})/RT) \tag{21}$$

where

$$V(R_{MM}) = \sum_{i=1}^{N_r}\sum_{j=1}^{N_o} Q_{ri}Q_{oj}e^2/D_sR_{ij}(R_{MM}) \tag{22}$$

Here, e is the charge of the electron, Q_{ri} is the net charge of the ith atom in the reduced species and Q_{oj} is that of the jth atom in the oxidized species. N_r stands for the total number of atoms in the reduced species and N_o is that in the oxidized species. $R_{ij}(R_{MM})$ is the distance between the ith and the jth atoms and is a function of R_{MM}. D_s is the static dielectric constant.

(iv) Calculational Details. Calculations were performed using GAUSSIAN 92 version E.1.[27] The procedure used for each species was, first, to optimize the geometries and to make a vibrational analysis, and then to scan its PES at the second-order Moller−Plesset perturbation theory (MP2) including full-orbital space electron correlation. The basis set used is the 6-311+G* standard basis. One of the difficulties in studying transition metal species is to determine the proper spin state. According to the ligand field theory, complexes with only a few ligands (and thus having only a weak "ligand field") should have high-spin ground state, thus we have studied $V^{3+}OH_2$ in its triplet and $V^{2+}OH_2$ in its quartet states. Because of the negligible structural change of ligand H_2O in optimization, the configuration of the ligand H_2O was kept the same as the optimized configuration of $M-OH_2$ in scanning the PES for every species by changing only the M−O bond length. The total energy $E(r)$ vs the M−O bond length r was calculated for every species, and then the obtained single-point energies were fitted to a higher power curve function.

$$E(r) = a_0 + a_1r + a_2r^2 + a_3r^3 + ... + a_nr^n + ... \tag{23}$$

Approximately, PES may also be expressed as an anharmonic oscillator potential (AOP) and the harmonic oscillator potential functions

$$E(q) = {}^1/_2 fq^2 - {}^1/_6\, gq^3 \tag{24}$$

$$E(q) = {}^1/_2\, fq^2 \tag{25}$$

TABLE 1: Optimized Geometrical Parameters and Force Constants at UMP2(full)/6-311+G* Level

	$V^{2+}OH_2$ ($^4B_2$)	$V^{3+}OH_2$ ($^3A_2$)	H_2O (free, $^1A_1$)
r_{M-O} (Å)	2.0562	1.7792	
r_{O-H} (Å)	0.9773	1.0425	0.9589 (0.9584)[a]
$\angle_{MOH}$ (degree)	127.08	126.59	
$\angle_{HOH}$ (degree)	105.84	106.82	107.66 (104.5)
f (mdyn/Å)	1.7555	4.1442	
g (mdyn/Å^2)	−6.5208	−21.6646	
Q_V	1.7721	2.3544	
Q_O	−0.8526	−0.6391	−0.7711
Q_H	0.5403	0.6425	0.3855

[a] The numbers in the parentheses in the column of species H_2O are referred to as the experimental values.

TABLE 2: Potential Energy Surface Constants and the Harmonic Frequencies of Several Low-Frequency Modes

$V^{2+}OH_2$		$V^{3+}OH_2$	
PES	frequencies	PES	frequencies
−0.113777104e4(a_0)[a]	547.83 (A1)[b]	−0.989833525e3(a_0)	699.75 (A1)
0.353511581e3(a_1)	904.73 (B2)	−0.615811974e2 (a_1)	1038.25 (B2)
−0.403206621e3(a_2)	931.03 (B1)	0.493336853e2 (a_2)	1042.37 (B1)
0.214247333e3(a_3)	1932.70 (A1)	−0.130965709e2(a_3)	1078.24 (A1)
−0.379954497e2(a_4)	3681.38 (B2)	−0.447131315e1(a_4)	2751.03 (B2)
−0.115572070e2(a_5)	3647.33 (A1)	0.395833254e1 (a_5)	2770.96 (A1)
0.608956959e1(a_6)		−0.100245684e1(a_6)	
−0.75461593 (a_7)		0.901884234e-1(a_7)	

[a] a_n ($n = 0, 1, 2, ...7$) are the coefficients of the accurately fitted PES (eq 23) and the corresponding units are a.u./Å^n. [b] The symbols in the parentheses in the frequency columns are referred to as the vibrational modes.

Substituting these PES functions into the activation energy formula and PES slope formula, the activation energy and the corresponding activation parameter and the PES slopes may be further obtained.

Analyses of the contact distance dependence of the relevant quantities (the coupling matrix element, the pair distribution function, and the electron transfer rate) are also made with 31 separated values of the contact distance (in a range from 3.5 to 11.0 Å). Finally, the numerical integral method makes eq 3 yield the total electron transfer rate. In addition, in the calculation of the pair distribution function, the net charges used for every atom were set to be equal to those of two isolated species (V^{2+}-OH_2 and $V^{3+}OH_2$) calculated with the optimized geometries.

To test the effect of the different ab initio calculation levels on the energy indexes, the activation energies and the bond-dissociation energy of the reactant molecules were also calculated at the different ab initio calculation levels. They include the Hartree−Fock self-consistent field (HF), MP2, MP3, MP4 with various excitations (MP4D, MP4DQ, MP4SDQ, MP4SDTQ), quadratic configuration interaction with single and double excitations (QCISD) and that with single, double, and triple excitations (QCISD(T)), and those with spin-projection (PMP2, PMP3). In these direct calculations of energy quantities, only the valence electrons are correlated.

3. Results and Discussion

The optimized molecular geometries, electronic charge distributions, force constants, and some relevant properties of the monohydrated transition metal ions $V^{2+}OH_2$ and $V^{3+}OH_2$ at the UMP2(full)/6-311+G* level have been summarized in Table 1. The fitted ab initio MP2(full)/6-311+G* PES and several low frequencies obtained at the HF/6-311+G* level are listed in Table 2. The relevant energy quantities (the total energy and the bond-dissociation energy of every species and the

TABLE 3: Various Energy Quantities at Different Theoretical Levels[a]

	species energies		dissociation energies		
methods	$E(V^{2+}OH_2)$	$E(V^{3+}OH_2)$	$D_e(V^{2+}OH_2)$	$D_e(V^{3+}OH_2)$	activation energy E_a
HF	−1018.288620	−1017.349955	104.44	137.00	4.0185
MP2(FC)	−1018.518674	−1017.597483	107.01	160.02	4.8510
MP3(FC)	−1018.523312	−1017.592185	106.11	154.66	4.5462
MP4D(FC)	−1018.527825	−1017.599846	105.74	156.85	4.7359
MP4DQ(FC)	−1018.526236	−1017.597367	105.64	156.14	4.8953
MP4SDQ(FC)	−1018.528459	−1017.606689	105.87	160.85	5.1542
MP4SDTQ(FC)	−1018.533709	−1017.621000	106.24	166.95	5.8610
QCISD(FC)	−1018.530377	−1017.617034	120.35	167.04	6.3180
QCISD(T,FC)	−1018.535291	−1017.629049	117.95	172.06	6.5491
PUHF	−1018.288725	−1017.350992	104.51	137.65	3.9285
PMP2(FC)	−1018.518726	−1017.598374	107.05	160.59	4.7566
PMP3(FC)	−1018.523403	−1017.593082			4.4430
MP2(full)	−1018.917645	−1018.000656	105.15	176.26	3.7970
PMP2(full)	−1018.918253	−1018.002522	105.40	177.10	3.6981
MP2(full)[b]					3.9935
MP2(full)[c]					4.2674
MP2(full)[d]					7.3931
quasi-expt[e]					1.508

[a] All methods are at the same basis set (6-311+G*) level. FC denotes the frozen-core approximation in the correlation calculation. In the parentheses, full denotes that the inner spheres are also included in the correlation calculation. All calculations of the activation energies are referred to the direct ones using the activation parameters unless noted otherwise. The units are in a.u. for E and in kcal/mol for D_e and E_a. [b] E_a is calculated using the activation model and the fitted accurate potential energy function (eq 23). [c] E_a is calculated using the activation model and the fitted AOP function (eq 24). [d] E_a is calculated using the classical George−Griffith formula with the calculated harmonic potential function (eq 25). [e] The quasiexperimental value is obtained from refs 28 and 29.

TABLE 4: The Contact Distance Dependence of Various Relevant Quantities

R_{VV} (Å)	$g(R_{VV})$	$H_{if}(R_{VV})$ (cm^{-1})	$\kappa_{el}(R_{VV})$
3.50	3.792116e-5	15576.24	1.000
3.75	6.994939e-5	12382.34	1.000
4.00	1.199899e-4	8223.32	1.000
4.25	1.938179e-4	4947.73	1.000
4.50	2.976930e-4	2789.37	1.000
4.75	4.381500e-4	1499.77	1.000
5.00	6.217984e-4	777.30	9.980e-01
5.25	8.551401e-4	391.07	8.592e-01
5.50	1.144412e-3	191.95	4.449e-01
5.75	1.495466e-3	92.25	1.393e-01
6.00	1.913666e-3	43.53	3.379e-02
6.25	2.403821e-3	20.22	7.437e-03
6.50	2.970149e-3	9.26	1.566e-03
6.75	3.616258e-3	4.18	3.204e-04
7.00	4.345132e-3	1.87	6.402e-05
7.25	5.159160e-3	0.83	1.253e-05
7.50	6.060126e-3	0.36	2.404e-06
7.75	7.049288e-3	0.16	4.536e-07
8.00	8.127376e-3	0.07	8.420e-08
8.25	9.294634e-3	0.03	1.540e-08
8.50	1.055089e-2	1.23e-2	2.778e-09
8.75	1.189558e-2	5.20e-3	4.947e-10
9.00	1.332778e-2	2.18e-3	8.706e-11
9.25	1.484621e-2	9.10e-4	1.515e-11
9.50	1.644942e-2	3.78e-3	2.608e-12
9.75	1.813564e-2	1.56e-4	4.445e-13
10.00	1.990291e-2	6.41e-5	7.505e-14
10.25	2.174916e-2	2.62e-5	1.266e-14
10.50	2.367207e-2	1.07e-5	1.998e-15
10.75	2.566933e-2	4.33e-6	4.441e-16
11.00	2.773846e-2	1.75e-6	0.000

activation energies) at different levels of theory and different electron correlation levels are collected in Table 3. The dependences of these relevant quantities on the contact distance are given in Tables 4−6 and are also shown in Figures 1−5, respectively. The calculated various parameters and the overall observed ET rates in gas phase and also in solution are given in Table 7.

(i) The Analysis of the Electronic Structural Properties of $V^{2+}OH_2$ and $V^{3+}OH_2$. Before we start to discuss the electron transfer reactivity and some kinetic properties of this electron self-exchange reaction system, $V^{2+}OH_2/V^{3+}OH_2$, it is very important to first analyze relevant electronic structures and properties.

Table 1 lists some structural parameters optimized at the UMP2(full)/6-311+G* level. No experimental value has been reported for the relevant structural parameters of this intermediate species with a few ligands. The ab initio calculations on the metal ion−water systems at the electron correlation level are expected to be able to give a basic understanding of the electronic structures and properties as well as to yield a reliable prediction of the relevant electron transfer kinetic parameters. Our theoretically optimized bond lengths at the UMP2(full)/6-311+G* level are 2.0562 Å ($V^{2+}OH_2$) and 1.7792 Å ($V^{3+}OH_2$) for the metal−oxygen separation (r_{M-O}). The results are significantly different from those of the hexaaquo metal ions, $V^{2+}(H_2O)_6$ and $V^{3+}(H_2O)_6$, found experimentally in the crystal state (2.260 Å in $V^{2+}(H_2O)_6$ and 2.070 Å in $V^{3+}(H_2O)_6$).[14] This observation may be attributed to no ligand−ligand repulsion interaction in these monohydrated metal ions and a stronger attraction interaction between the V^{2+} or V^{3+} and H_2O molecules in the monohydrated systems than that in the hexaaquo systems. The V−O bond length of the $V^{2+}OH_2$ species is slightly shorter by 0.086 Å than that of $V^{+}OH_2$ species calculated by Rosi and Bauschlicher at the electron correlation level using the modified coupled pair functional method with a larger basis set.[28] The fully optimized O−H bond lengths for those two species are slightly longer by 0.018 Å in $V^{2+}OH_2$ and by 0.084 Å in $V^{3+}OH_2$ than that in the free state of H_2O optimized at same level of theory and also than the experimental value, while the optimized HOH angles of both species are very close to the results of H_2O in the free state calculated at same level of theory and also very close to the experimental value of H_2O in the free state. This observation has indicated that formation of the V−O bond in both species ($V^{2+}OH_2$ and $V^{3+}OH_2$) results in the transfer of part of a charge from the ligand H_2O, especially for O, to V^{2+} or V^{3+} ions. This charge transfer weakens the O−H bond strength and leads the O−H bond to become longer than that in the H_2O free state. The more

TABLE 5: The Contact Distance Dependence of the Electron Transfer Rate (M^{-1} s^{-1})

	$k_{et}(R_{VV}/gas$			$k_{et}(R_{VV})$/solution		
R_{VV}	accurate	AOP	G−G	accurate	AOP	G−G
3.50	.1191E+10	.7504E+09	.3860E+07	.4057E+03	.2556E+03	.1315E+01
3.75	.1191E+10	.7504E+09	.3860E+07	.4057E+03	.2556E+03	.1315E+01
4.00	.1191E+10	.7504E+09	.3860E+07	.4057E+03	.2556E+03	.1315E+01
4.25	.1191E+10	.7504E+09	.3860E+07	.4057E+03	.2556E+03	.1315E+01
4.50	.1191E+10	.7504E+09	.3860E+07	.4057E+03	.2556E+03	.1315E+01
4.75	.1191E+10	.7504E+09	.3860E+07	.4057E+03	.2556E+03	.1315E+01
5.00	.1189E+10	.7497E+09	.3857E+07	.4049E+03	.2552E+03	.1313E+01
5.25	.1042E+10	.6647E+09	.3419E+07	.3485E+03	.2224E+03	.1144E+01
5.50	.5549E+09	.3615E+09	.1859E+07	.1805E+03	.1174E+03	.6039E+00
5.75	.1769E+09	.1168E+09	.6007E+06	.5653E+02	.3721E+02	.1914E+00
6.00	.4315E+08	.2862E+08	.1472E+06	.1371E+02	.9060E+01	.4661E−01
6.25	.9511E+07	.6315E+07	.3249E+05	.3017E+01	.1996E+01	.1027E−01
6.50	.2003E+07	.1331E+07	.6845E+04	.6353E+00	.4204E+00	.2163E−02
6.75	.4099E+06	.2723E+06	.1401E+04	.1300E+00	.8602E−01	.4425E−03
7.00	.8190E+05	.5440E+05	.2798E+03	.2597E−01	.1719E−01	.8840E−04
7.25	.1602E+05	.1064E+05	.5475E+02	.5081E−02	.3363E−02	.1730E−04
7.50	.3076E+04	.2043E+04	.1051E+02	.9754E−03	.6455E−03	.3320E−05
7.75	.5803E+03	.3855E+03	.1983E+01	.1840E−03	.1218E−03	.6264E−06
8.00	.1077E+03	.7155E+02	.3681E+00	.3416E−04	.2260E−04	.1163E−06
8.25	.1970E+02	.1309E+02	.6732E−01	.6247E−05	.4134E−05	.2127E−07
8.50	.3554E+01	.2361E+01	.1214E−01	.1127E−05	.7458E−06	.3836E−08
8.75	.6330E+00	.4204E+00	.2163E−02	.2007E−06	.1328E−06	.6832E−09
9.00	.1114E+00	.7398E−01	.3805E−03	.3532E−07	.2337E−07	.1202E−09
9.25	.1938E−01	.1287E−01	.6622E−04	.6145E−08	.4066E−08	.2092E−10
9.50	.3337E−02	.2216E−02	.1140E−04	.1058E−08	.7002E−09	.3602E−11
9.75	.5688E−03	.3778E−03	.1943E−05	.1803E−09	.1194E−09	.6140E−12
10.00	.9599E−04	.6382E−04	.3283E−06	.3045E−10	.2015E−10	.1037E−12
10.25	.1613E−04	.1066E−04	.5486E−07	.5134E−11	.3349E−11	.1723E−13
10.50	.2644E−05	.1833E−05	.9429E−08	.8107E−12	.5676E−12	.2920E−14
10.75	.5289E−06	.3333E−06	.1714E−08	.1802E−12	.1135E−12	.5840E−15
11.00	.0000E+00	.0000E+00	.0000E+00	.0000E+00	.0000E+00	.0000E+00

TABLE 6: The Contact Distance Dependence of the Sphere Averaged Electron Transfer Rate $\langle k_{et}\rangle_s$ at a Fixed Contact Distance

	sphere averaged $\langle k_{et}\rangle_s$/gas			sphere averaged $\langle k_{et}\rangle_s$/solution		
R_{VV}	accurate	AOP	G−G	accurate	AOP	G−G
3.50	.4885E+04	.3078E+04	.1583E+02	.1664E−02	.1049E−02	.5394E−05
3.75	.1108E+05	.6984E+04	.3593E+02	.3775E−02	2379E−02	.1224E−04
4.00	.2307E+05	.1454E+05	.7479E+02	.7860E−02	.4953E−02	.2548E−04
4.25	.4470E+05	.2817E+05	.1449E+03	.1523E−01	.9596E−02	.4936E−04
4.50	.8150E+05	.5136E+05	.2642E+03	.2776E−01	.1750E−01	.9000E−04
4.75	.1411E+06	.8890E+05	.4573E+03	.4806E−01	.3028E−01	.1558E−03
5.00	.2332E+06	.1470E+06	.7562E+03	.7939E−01	.5005E−01	.2575E−03
5.25	.3252E+06	.2075E+06	.1067E+04	.1088E+00	.6943E−01	.3571E−03
5.50	.2666E+06	.1736E+06	.8932E+03	.8670E−01	.5639E−01	.2901E−03
5.75	.1269E+06	.8376E+05	.4309E+03	.4055E−01	.2669E−01	.1373E−03
6.00	.4500E+05	.2985E+05	.1535E+03	.1430E−01	.9449E−02	.4860E−04
6.25	.1408E+05	.9350E+04	.4810E+02	.4467E−02	.2955E−02	.1520E−04
6.50	.4123E+04	.2738E+04	.1409E+02	.1307E−02	.8652E−03	.4450E−05
6.75	.1150E+04	.7640E+03	.3930E+01	.3647E−03	.2413E−03	.1241E−05
7.00	.3080E+03	.2046E+03	.1052E+01	.9765E−04	.6462E−04	.3324E−06
7.25	.7948E+02	.5280E+02	.2716E+00	.2520E−04	.1668E−04	.8579E−07
7.50	.1984E+02	.1318E+02	.6779E−01	.6292E−05	.4163E−05	.2142E−07
7.75	.4804E+01	.3191E+01	.1641E−01	.1523E−05	.1008E−05	.5185E−08
8.00	.1131E+01	.7512E+00	.3864E−02	.3586E−06	.2373E−06	.1221E−08
8.25	.2594E+00	.1723E+00	.8864E−03	.8226E−07	.5444E−07	.2800E−09
8.50	.5810E−01	.3859E−01	.1985E−03	.1842E−07	.1219E−07	.6271E−10
8.75	.1273E−01	.8453E−02	.4348E−04	.4035E−08	.2670E−08	.1374E−10
9.00	.2730E−02	.1813E−02	.9328E−05	.8657E−09	.5729E−09	.2947E−11
9.25	.5745E−03	.3816E−03	.1963E−05	.1822E−09	.1205E−09	.6201E−12
9.50	.1187E−03	.7886E−04	.4057E−06	.3765E−10	.2491E−10	.1281E−12
9.75	.2412E−04	.1602E−04	.8241E−07	.7648E−11	.5062E−11	.2604E−13
10.00	.4820E−05	.3205E−05	.1648E−07	.1529E−11	.1012E−11	.5205E−14
10.25	.9532E−06	.6302E−06	.3242E−08	.3034E−12	.1979E−12	.1018E−14
10.50	.1828E−06	.1267E−06	.6519E−09	.5605E−13	.3924E−13	.2019E−15
10.75	.4255E−07	.2681E−07	.1379E−09	.1449E−13	.9133E−14	.4698E−16
11.00	.0000E+00	.0000E+00	.0000E+00	.0000E+00	.0000E+00	.0000E+00

the positive charge on the metal V ion, the greater the charge transfer magnitude and the longer the O−H bond in the monohydrated ion. However, the binding interaction between the metal vanadium ion and H_2O does not significantly change the angle between two O−H bonds. The electronic charge distribution given in Table 1 has fully shown this charge transfer phenomenon in the formation of $V^{2+}OH_2$ and $V^{3+}OH_2$ species.

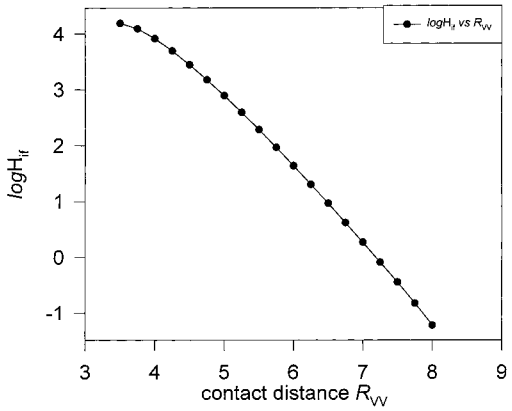

Figure 1. The contact distance dependence of the coupling matrix element logH_{if}.

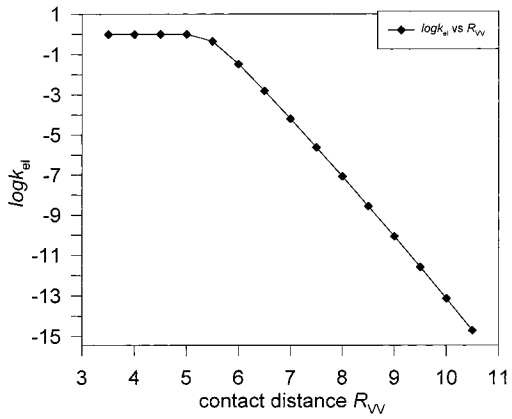

Figure 2. The contact distance dependence of the electronic transmission coefficient logk_{el}.

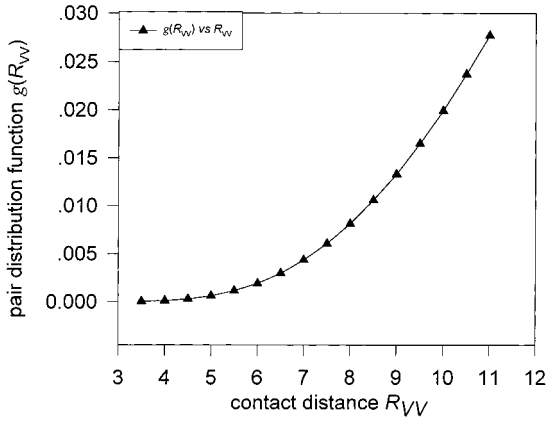

Figure 3. The contact distance dependence of the pair distribution function $g(R_{VV})$.

As the UMP2(full)/6-311+G* calculations yield only a small distortion of the H_2O geometry from the optimized geometry in scanning PES because of its interaction with the metal ion, the H_2O geometry was fixed at its optimized configuration, and only the V−O distance was scanned in determining PESs of $V^{2+}OH_2$ or $V^{3+}OH_2$. Since UMP2(full)/6-311+G*optimizations on these two species show the molecule to be planar, we constrain a water molecule and vanadium atom to be in a plane. Therefore, all of the systems have been considered a planar, yielding C_{2v} symmetry for $V^{2+}OH_2$ and $V^{3+}OH_2$, and the PESs of these two species become of one-dimension. The fitted coefficients of the one-dimensional potential energy surface that occurred in eq 23 have been given in Table 2. Table 2 also lists the harmonic vibrational frequencies of six low-frequency

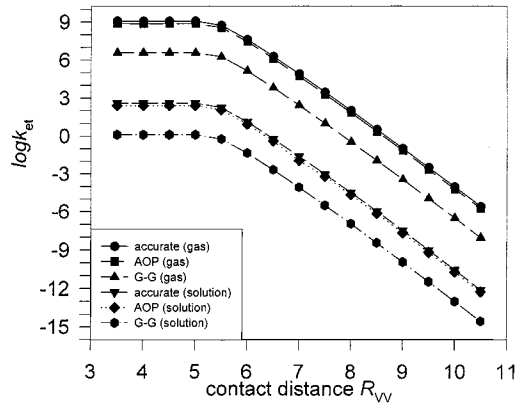

Figure 4. The contact distance dependence of the ET rate logk_{et}.

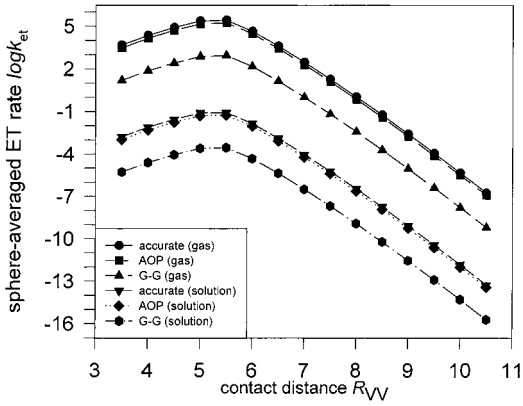

Figure 5. The contact distance dependence sphere-averaged ET rate logk_{et}.

modes for these two species. Obviously, the later three vibrational modes for each species correspond to the harmonic vibrational modes of the H_2O molecule in the free state with different shifts. The frequencies corresponding to the modes of the H_2O molecule in $V^{2+}OH_2$ species (1932.70(A1), 3647.33-(A1), and 3681.38(B2) cm^{-1}) are slightly greater than those of the H_2O molecule in the free state(1861.59(A1), 3867.60(A1), and 3970.08(B2)cm^{-1}). But in $V^{3+}OH_2$ species, the harmonic vibrational modes of H_2O after combining with V^{3+} ion have larger shifts, the vibrations change from the higher frequencies (1861.59(A1), 3867.60(A1), and 3970.08(B2) cm^{-1}) to the lower frequencies (1078.24(A1), 2770.96(A1), and 2751.03(B2) cm^{-1}). This phenomenon has indicated that there is a stronger binding interaction between V^{3+} and ligand H_2O than that between V^{2+} and ligand H_2O. In other words, V^{3+} with stronger attracting electron ability makes a great charge transfer from H_2O to V^{3+}. This transfer greatly weakens the bonds in the H_2O molecule and finally cause the shifts of the vibrations of ligand H_2O to the lower frequencies. The first frequencies ($V^{2+}OH_2$: 547.83(A1) and $V^{3+}OH_2$: 699.75(A1) cm^{-1}) of both species correspond to the compression-stretching vibrations between the metal ion (V^{2+} or V^{3+}) and the ligand H_2O, and other two groups of frequencies ($V^{2+}OH_2$: 904.73(B1), 931.03(B2) and $V^{3+}OH_2$: 1038.25(B2), 1042.37(B1) cm^{-1}) correspond to two bend vibrational modes. Actually, the first A1 vibrational mode for every species reflects the strength of the V−O bond. These values (547.83 cm^{-1} for $V^{2+}OH_2$ and 699.73 cm^{-1} for V^{3+}-OH_2) are significantly different from those of the V−O bond stretching−compression vibrations of the corresponding hexaaquo systems in the crystal ($V^{2+}(H_2O)_6$: ∼389.0 cm^{-1} and V^{3+}-$(H_2O)_6$: ∼480.0 cm^{-1}).[20] This observation has implied that as there is no ligand−ligand repulsion interaction in the monohydrated species, the interaction between the metal ion and the

TABLE 7. Various Activation Kinetics Parameters of the $V^{2+}OH_2/V^{3+}OH_2$ System

	accurate[a]	AOP[b]	G−G[c]	INDO/II	others
activation M−O bond length r^t (Å)	1.8842				
$E_{ad,in}$ (kcal/mol)	3.9935	4.2674	7.3931		
$E_{ad,out}$ (kcal/mol)					8.833[d]
$\|S_2 - S_1\|_{in}$ (erg/cm)	1.12e-3	1.06e-3		2.60e-4	5.77e-4[e]
$\|S_2 - S_1\|_{out}$ (erg/cm)					0.83e-4
k_{et}(gas) ($M^{-1}s^{-1}$)	1.94e5	1.24e5	6.38e2		
k_{et}(solution) ($M^{-1}s^{-1}$)	6.46e-2	4.13e-2	2.12e-4		

[a] Using eq 23. [b] Using eq 24. [c] Using eq 25. [d] From the continuum medium model. The effective radii used are 2.57 Å for $V^{2+}OH_2$ and 2.53 Å for $V^{3+}OH_2$, respectively. [e] From eq 18.

ligand is stronger than that in the hexaaquo species, thus the vibrations must shift to the higher frequencies. This trend agrees well with the above analysis about the molecular geometries and the electronic charge distribution. Similarly, the dissociation energies in Table 3 also support the above analysis. In addition, from Table 3, it should be noted that UHF calculations give poor dissociation energy results. Inclusion of the electron correlation significantly lowers the total energies of these systems by about 150.0kcal/mol and increases the dissociation energies. Especially for $V^{3+}OH_2$ species, the electron correlation effect is very evident. The results at several Moller−Plesset perturbation theory levels are in good agreement with each other. They are very close to those obtained using the quadratic configuration interaction (QCI) method with single and double substitutions or with single, double, and triple substitutions. Comparison of the data at full electron correlation level with those at the valence electron correlation level indicates that the full electron correlation method gives greater dissociation energies than the valence electron correlation method. Annihilation of the first spin contaminant by using the spin-projection method can slightly increase the dissociation energies.

The above analysis has indicated that the second-order Moller−Plesset perturbation theory can give more reasonable results for these monohydrated species and is suitable for the further approaches to the electron transfer kinetic problem.

(ii) Electronic Factor. In the calculation of the electronic transmission coefficient, two key quantities are H_{if} and the PES slope difference.

For the PES slopes of the hydrated system, no accurate treatment has been given and some simplified forms are usually used in many recent works. Khan's study used equivalent M−L bond length change from the initial state to the transition state for both the reduced and the oxidized species to calculate the PES slopes.[29] Actually, these two bond length changes are unequivalent. Early investigations have shown that the r_{M-L} change of the reduced species is generally about 1.5 times more than that of the oxidized species.[20] For the $V^{2+}OH_2/V^{3+}OH_2$ system, the q_r^t/q_o^t ratio is 1.438. Therefore, in discussing ET kinetics by means of the Landau−Zener principle, the PES slopes should be accurately determined.

Table 7 also compares relevant results of the PES slopes obtained using several different methods. It is observed that the slopes ($|S_2 - S_1|$) from the accurate method are in very good agreement with those from the anharmonic oscillator potential (AOP) method and are higher than those obtained from the approximate method (eq 18) and from the INDO/II method. This observation may be interpreted as the fact that these ab initio PESs take fully into account the interaction between the metal ion and the ligand H_2O and the semiempirical INDO/II method takes into account only the partial bonding contribution due to the electronic overlap between the metal ion and ligand.

For the coupling quantity, the two-state model is valid, but this model needs accurate initial and final state functions which are difficult to determine for the hydrated systems. In this work, we simplify the procedure and divide the hydrated ion into the inner-sphere complex ion and the outer-sphere medium and make calculations only on the inner-sphere ion. The presented method is based on the Slater-type d-electron wave functions of the metal ion and the perturbation theory and takes into account not only the d-type molecular orbital overlap interaction of the hydrated ion but also the effect of the outer-sphere solvent medium. It should be a reliable method.

The dependence of the coupling matrix element H_{if} on the contact distance R_{MM} has been demonstrated in Figure 1. It is obviously observed that the plot of $\log H_{if}$ vs R_{VV} is mostly linear and the coupling matrix element H_{if} rapidly decays along with the increase of the contact distance. The shorter the contact distance, the greater the coupling matrix element. When $R_{VV} < 4.8$ Å, $H_{if} > 1000$ cm^{-1}, while when $R_{VV} > 7.0$ Å, $H_{if} < 1.0$ cm^{-1} and mostly tends toward zero. Thus, from this observation we can know that the effective electronic coupling requires the contact distance smaller than 7.0 Å.

The electronic transmission coefficient κ_{el} has been calculated in terms of the PES slopes and the H_{if} values, and its contact distance dependence is plotted in Figure 2. Results have indicated that when $R_{VV} < 5.0$ Å, $\kappa_{el} \sim 1.0$ and when $R_{VV} > 7.5$ Å, $\kappa_{el} < 1e-6$. In the range from 5.0 to 7.5 Å, κ_{el} exponentially decays along with the increase of the contact distance. Thus, for this reacting system the ET reactions in the range greater than 5.0 Å of the contact distance are nonadiabatic in nature. This indicates that the early assumption in which κ_{el} is approximately taken as unity is not correct. This electronic factor should be accurately taken into account in determining the ET rate and other kinetic parameters.

(iii) Activation Energy. At the present time, no experimental activation energies have been reported for this kind of ET reaction involving the monohydrated ion pairs. Its quasiexperimental values may be evaluated as $^1/_6$ of the activation energy of the hexaaquo system. Because of the differences of the PESs and the geometrical parameters between the monohydrated and the hexaaquo systems, such an evaluated quasiexperimental activation energy actually is approximate and can be taken only as a reference value.

Comparison of the activation energy data in Table 3 shows that the values obtained from the accurate potential (eq 23) are in good agreement with those obtained from AOP (eq 24), and all of them are slightly greater than and close to the quasiexperimental value. They differ significantly from those obtained from the George−Griffith formalism[30] which neglects the anharmonic feature of the PESs. This analysis is also in agreement with the early conclusion in the previous works.[10] Further, the observed reasonable agreement between the theoretical and the quasiexperimental values fully indicates that the activation model presented in this work is very valid in determining the activation energy of electron self-exchange reaction. This activation model avoids some shortcomings of

the classical model and utilizes the more accurate potential functions, including the anharmonic feature of the PES to calculate the activation energy, and should be a reliable method.

To test the effect of the calculational level of theory on the activation energy, the activation energies also are directly calculated from the energy difference of the reacting system between the initial state and the transition state by using different valence electron correlation methods. In these calculations, the activation parameters used are gotten from the activation model. These results are summarized in Table 3. It is first noted that the activation energy at the unrestricted Hartree−Fock level is slightly smaller than those at the electron correlation level. The frozen-core (FC) MP2 value is slightly greater than the MP3-(FC) value. Both of them are mostly smaller than all of the fourth-order MP4(FC) results, except for the MP4D(FC) value which is slightly smaller than the MP2(FC) value. For the MP4-(FC) calculations, the activation energies depend on the number of substitution types. Namely, the activation energies increase according to the following order: MP4D < MP4DQ < MP4SDQ < MP4SDTQ. The greatest MP4SDTQ(FC) value of all data at the fourth MP level is slightly smaller than and very close to those at the quadratic configuration interaction (QCI) level. Similarly, the QCISD(T) activation energy value including a perturbational estimate of the connected triple excitations is slightly greater than the QCISD value.

Comparison among full-electron correlation MP2 values indicates that the results from the direct calculation method are in excellent agreement with those from the activation model with the accurately fitted potential function and are very close to those from the activation model with the fitted AOP function. This observation further confirms that the activation model presented here is very reasonable and that the accurate anharmonic PES is very important for the analysis of the electron transfer kinetics problem.

In addition, inclusion of the inner spheres in the electron correlation calculation may effectively decrease the activation energy (comparing UMP2(full) and PMP2(full) data (3.7970 and 3.6981kcal/mol) with UMP2(FC) and PMP2(FC) data (4.8510 and 4.7566kcal/mol)). Annihilation of the first spin contaminant by using the spin-projection method can led to pure-state PMP2 energy values. Comparison between MP2 and PMP2 values has indicated that the activation energies at various electron correlation levels after annihilation of the spin contaminant are slightly smaller than those before annihilating the spin contaminant.

(iv) Pair Distribution Function. Table 4 gives some discrete data for the pair distribution function at the different contact distances. The fitted smooth change of the pair distribution function along the contact distance has been demonstrated in Figure 3. It can be seen from Figure 3 and Table 4 that $g(R_{VV})$ increases with R_{VV}. The shorter the contact distance, the smaller the pair distribution function. Its values are from $1e-2$ to $1e-5$ in the range of $12.0 \sim 3.5$ Å of the contact distance. The observation has indicated that the interaction between two reacting species in the encounter process is the repulsive one, and it actually corresponds to the work bringing two reacting species together to form an encounter complex. Thus, this distribution function is actually proportional to the preequilibrium constant. Obviously, the contribution from the pair distribution function to total rate constant is inversely dependent on R_{VV}.

(v) ET Rate. A number of rate constant values have been obtained at the different contact distances. The R_{VV} dependence of the electron transfer rate has been drawn out in Figure 4 for three theoretical methods and two phase-state processes. From Figure 4 and relevant calculated results, it can be known that k_{et} tends to a maximum constant value where $R_{VV} < 4.7$ Å. After 5 Å of the contact distance, k_{et} rapidly decreases with R_{VV}. When $R_{VV} > 8.0$ Å, k_{et} has decreased by about seven orders of magnitude. This rate change is mainly attributed to contribution from the electronic factor. Taking into account the pair distribution function, the averaged electron transfer rate ($\langle k_{et} \rangle_s$) in a spherical volume element with R_{VV} of radius at a fixed R_{VV} value obviously falls off. The contact distance dependence of this averaged rate has been drawn out in Figure 5. In particular, when $R_{VV} < 5.0$ Å, the rate of fall off is greater than that when $R_{VV} > 5.0$ Å. At $R_{VV} \approx 5.3$ Å, there is a maximum contribution (accurate: 3.25e5 $M^{-1}s^{-1}$, gas) of $\langle k_{et} \rangle_s$ (in a fixed volume element) to the total ET rate. This value is very close to the total observed ET rate values (accurate: 1.94e5 $M^{-1}s^{-1}$). Good agreement of the theoretical values from the accurate potential method with those from AOP method may be observed from Tables 5−6 for both the gas phase and the solution processes. They are obviously greater than those obtained using the harmonic potential function and the George−Griffith formalism. For these systems, the ET rates in the gaseous process are generally about 10^5 $M^{-1}s^{-1}$, while the rates in solution are only about 10^{-2} $M^{-1}s^{-1}$. This phenomenon has demonstrated that the solvent effect is very important.

In conclusion, good agreement between them has indicated that the presented theoretical scheme is very valid. Further, since it is impossible to experimentally determine the structures and their PESs of these hydrated systems, especially for the unstable intermediate species, ab initio calculations can play an effective auxiliary part in discussing the ET reactivities of these kinds of reacting systems.

Acknowledgment. This work was supported by the National Natural Science Foundation of China and the Natural Science Foundation of Shandong province.

References and Notes

(1) Marcus, R. A.; Sutin, N. *Biochim. Biophys. Acta* **1985**, *811*, 265.
(2) Marcus, R. A. *J. Chem. Phys*. **1956**, *24*, 966; **1965**, *43*, 679, 3477. Marcus, R. A. *Faraday Discuss. Chem. Soc.* **1982**, *74*, 7.
(3) Hush, N. S.; *Trans. Faraday Soc.* **1961**, *57*, 557; *Electrochim. Acta* **1968**, *13*, 1005.
(4) Sutin, N. *Annu. Rev. Nucl. Sci.* **1962**, *12*, 285; *Prog. Inorg. Chem.* **1983**, *30*, 441; *Trans. Faraday Soc*. **1965**, *57*, 155.
(5) Hupp, J. T.; Weaver, M. J. *J. Phys. Chem.* **1985**, *89*, 2795; **1990**, *94*, 8608.
(6) Newton, M. D.; Sutin, N. *Annu. Rev. Phys. Chem.* **1984**, *35*, 437.
(7) Cannon, R. D. *Electron Transfer Reaction*; Butterworth: London, 1980. Sutin, N. *In Progress in Inorganic Chemistry*; Lippard, S. J.; Ed., Wiley: New York, 1982; Vol. 30.
(8) Tunuli, M. S.; Khan, S. U. M. *J. Phys. Chem.* **1987**, *91*, 3474.
(9) Bockris, J. O'M.; Khan, S. U. M. *Quantum Electrochemistry*; Plenum Press: New York, 1979.
(10) Bu, Y. *J. Phys. Chem.* **1994**, *98*, 2290.
(11) Bu, Y.; Song, X. *J. Phys. Chem*. **1994**, *98*, 5049.
(12) Bu, Y. *J. Phys. Chem*. **1995**, *99*, 11650.
(13) Bu, Y.; Deng, C. *J. Phys. Chem.* **1996**, *100*, 18093.
(14) Bu, Y.; Ding, Y.; He, F.; Jiang, L.; Song, X. *Int. J. Quantum Chem.* **1997**, *61*, 117.
(15) Bu, Y. *J. Mol. Struct. (THEOCHEM)* **1994**, *309*, 121.
(16) Bu, Y.; Wang, B. *J. Mol. Struct. (THEOCHEM)* **1994**, *313*, 275.
(17) Bu, Y.; Song, X.; Deng, C. *J. Mol. Struct.* (THEOCHEM) **1995**, *358*, 211.
(18) Bu, Y.; Song, X.; Deng, C. *Chem. Phys. Lett.* **1996**, *250*, 455.
(19) Bu, Y.; Liu, S.; Song, X. *Chem. Phys. Lett.* **1994**, *227*, 121.
(20) Bu, Y.; Deng, C.; Song, X. *Chem. Res. Chin. Univ*. **1995**, *11*(2), 137.
(21) Bu, Y.; Deng, C. *J. Phys. Chem.* **1997**, *101*, 1198.

(22) Bu, Y.; Xu, F.; Deng, C. *J. Mol. Struct. (THEOCHEM)*, **1997**, *392*, 141.

(23) Newton, M. D. *Int. J. Quantum Chem., Quantum Chem. Symp*. **1980**, *14*, 363.

(24) Newton, M. D. *J. Chem. Phys.* **1983**, *78*, 4086; **1982**, *76*, 1490.

(25) Landau, L. *Phys. Z. Sowjet* **1932**, *2*, 6.

(26) Zener, C. *Proc. R. Soc. London Ser.* **1932**, *A137*, 696; **1933**, *140*, 660.

(27) *Gaussian 92, Revision E.1*; Frisch, M. J.; Trucks, G. W.; Head-Gordon, M.; Gill, P. M. W.; Wong, M. W.; Foresman, J. B.; Johnson, B. G.; Schlegel, H. B.; Robb, M. A.; Replogle, E. S.; Gomperts, R.; Andres, J. L.; Raghavachari, K.; Binkley, J. S.; Gonzalez, C.; Martin, R. L.; Fox, D. J.; Defrees, D. J.; Baker, J.; Stewart, J. J. P.; Pople, J. A. Gaussian, Inc.: Pittsburgh, PA, 1992.

(28) Rosi, M.; Bauschlicher, C. W., Jr. *J. Phys. Chem.* **1989**, *90*, 7264.

(29) Khan, S. U. M.; Zhou, Z. *J. Chem. Phys.* **1990**, *93*, 8809.

(30) George, P.; Griffith, J. S. In *The Enzymes*; Boyer, P. D., Lardy, H., Myrback, N., Eds.; Academic: New York, 1955; Vol. 1, Chapter 8, p 347.